

# Electromagnetically Induced Transparency in optically trapped rubidium atoms

Bernd Kaltenhäuser,\* Harald Kübler, Andreas Chromik, Jürgen Stuhler, and Tilman Pfau  
5. *Physikalisches Institut, Universität Stuttgart, 70550 Stuttgart, Germany.*†

Atac Imamoglu  
*Institute of Quantum Electronics, ETH-Zürich, 8093 Zürich, Switzerland*

We demonstrate electromagnetically induced transparency (EIT) in a sample of rubidium atoms, trapped in an optical dipole trap. Mixing a small amount of  $\sigma^-$ -polarized light to the weak  $\sigma^+$ -polarized probe pulses, we are able to measure the absorptive and dispersive properties of the atomic medium at the same time. Features as small as 4 kHz have been detected on an absorption line with 20 MHz line width.

PACS numbers:

## INTRODUCTION

Electromagnetically induced transparency allows for the elimination of absorption in an otherwise opaque medium [1]. The effect is based on a third state, which is coupled to the excited state by an additional laser, such that all possible absorption paths destructively interfere. On the level of single excitations, the corresponding collective excitations can be described as a quasi-particle, the so-called dark state polariton [2]. Recently, the particle nature of dark state polaritons has been experimentally demonstrated [3].

In quantum information processing, photons can be used as robust information carriers [4], but they lack the possibility of storage. To overcome this shortcoming, several experiments have used the concept of dark state polaritons to store photonic information in cold atoms [5] and vapor cells [6]. Furthermore, as a step towards storage in a solid, EIT has been demonstrated in a room-temperature solid [7]. It has also been shown theoretically that EIT in atomic ensembles can be used to enhance the possibilities of long-distance quantum communication [8].

Spin squeezing is often regarded as a benchmark for the control of atom-light-states. This effect has already been demonstrated in a vapor cell via a quantum nondemolition measurement [9]. In magneto-optically trapped cold atoms it has been demonstrated in a similar way [10], as well as by mapping the squeezed state of light onto the atomic ensemble[11]. Recently, de Echaniz and co-workers have shown that this effect can be significantly increased in an optical dipole trap [12].

Here, we report on the first experimental demonstration of EIT in an optical dipole trap. Contrary to magneto-optical and magnetic traps, our setup allows for arbitrary magnetic fields. A homogeneous magnetic field can be used to address different magnetic substates of the medium.

We have measured 4 kHz features in the EIT response. This is an important step towards long storage times of quantum information in an atomic ensemble and the investigation of trapped darkstate polaritons.

## EXPERIMENTAL SETUP

To prepare an absorbing medium of trapped atoms, we first capture  $4 \cdot 10^9$  Rb-87 atoms in a magneto-optical trap. Afterwards, we apply a Dark-MOT phase (DM) for 25 ms to ensure an efficient transfer of the atoms to the dipole trap. For the DM, we ramp up the magnetic gradient field from 13.7 to 18 G/cm, detune the MOT-lasers to  $-100$  MHz from resonance and lower the repump laser power to 1%. After the DM we have  $7 \cdot 10^8$  atoms at a temperature of  $38 \mu\text{K}$  and a density of  $10^{12} \text{ atoms}\cdot\text{cm}^{-3}$  left.

The crossed CO<sub>2</sub>-laser dipole trap (DT) is turned on during the loading steps described above. After switching off the DM and additional 80 ms thermalization time we capture  $2 \cdot 10^7$  atoms at a density of  $2 \cdot 10^{11} \text{ atoms}\cdot\text{cm}^{-3}$  in the DT. Due to optical pumping, the atoms are distributed over the 5 magnetic substates of the  $5S_{1/2}$ ,  $F = 2$  ground state. Because the potential of the DT is much steeper than the one of the DM, the cloud heats up to a temperature of  $110 \mu\text{K}$ . The cloud provides a medium with an optical density up to 0.76 for a single Zeeman component on resonance.

For the EIT-measurements, a magnetic offset field of 129 G is applied parallel to the laser beam propagation. At this field strength, the magnetic substates of the  $5S_{1/2}$  ground state can be addressed individually. This allows to perform the EIT-measurement only between the ( $5S_{1/2}$ ,  $F = 2$ ,  $m_F = -1$ ) and ( $5S_{1/2}$ ,  $F = 1$ ,  $m_F = +1$ ) substates. We use a Raman laser system to address these transitions, which are shown in figure 1.

The setup for the EIT-measurements is shown in figure 2.

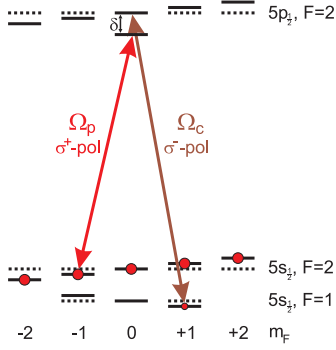


FIG. 1: Level scheme of the EIT transition. The probe laser couples to the  $5S_{1/2}, F = 2, m_F = -1 \leftrightarrow 5P_{1/2}, F = 2, m_F = 0$  transition, the coupling laser to the  $5S_{1/2}, F = 2, m_F = +1 \leftrightarrow 5P_{1/2}, F = 2, m_F = 0$  transition.

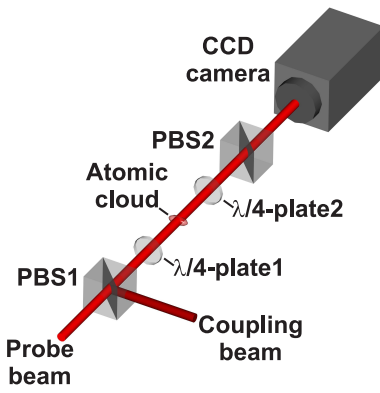


FIG. 2: Setup for the experiment: the probe and the coupling laser are overlapped in a polarizing beamsplitter (PBS). With the following  $\lambda/4$ -plate the polarization of the pulses are adjusted before they enter the cloud. With the second  $\lambda/4$ -plate the polarizations are turned again to separate the probe from the coupling beam in the following polarizing beamsplitter. Due to lenses (not shown in the picture), the cloud is imaged onto a high efficiency CCD camera.

For revealing the dispersive properties of the medium, the first  $\lambda/4$ -plate is turned, until a  $\sigma^-$ -polarized intensity admixture of  $a^2 = 8.7\%$  to the probe beam is obtained. The second  $\lambda/4$ -plate compensates this effect and mixes both polarizations back to linearly polarized light, which is then measured beyond the second polarizing beamsplitter. This causes the two polarizations to interfere. A similar method has recently been demonstrated with a vapor cell in a Sagnac interferometer [13]. Due to the large Zeeman-shift of the magnetic substates, the Raman-condition is not fulfilled for the wrong polarizations and thus the admixture in the coupling beam can be neglected.

## THEORY

As described above, the first  $\lambda/4$ -plate mixes a relative intensity  $a^2$  of  $\sigma^-$ -polarization into the otherwise  $\sigma^+$ -polarized probe beam. Due to birefringence in the optical viewports of the vacuum chamber, the  $\sigma^-$ -polarized beam collects an additional phase  $\phi$  relative to the  $\sigma^+$ -polarized beam. The total electric field acting on the atoms can then be described via

$$\begin{aligned} |E_{in}|^2 &= |E_{in,\sigma^+} + E_{in,\sigma^-}|^2 \\ &= \left| \sqrt{1-a^2} E_0 + a E_0 \exp\{i\phi\} \right|^2 \\ &= E_0^2 \left( 1 + 2a\sqrt{1-a^2} \cos\phi \right). \end{aligned} \quad (1)$$

When we tune the coupling laser to resonance, the single-photon and two-photon detuning of the probe laser become identical and the susceptibility for the  $\sigma^+$ -polarized probe laser is given by [14]

$$\begin{aligned} \chi^{(+)} &= \frac{|\mu|^2 \varrho}{\epsilon_0 \hbar} \\ &\times \left[ \frac{4\delta(\Omega_c^2 - 4\delta^2 - \gamma^2)}{|\Omega_c^2 + (\Gamma + i2\delta)(\gamma + i2\delta)|^2} \right. \\ &\left. + i \frac{8\delta^2 \Gamma + 2\gamma(\Omega_c^2 + \gamma\Gamma)}{|\Omega_c^2 + (\Gamma + i2\delta)(\gamma + i2\delta)|^2} \right]. \end{aligned} \quad (2)$$

To derive this equation, we have also assumed that the relevant atomic population stays mainly in the initial  $5S_{1/2}, F = 2, m_F = -1$  state. This is fulfilled, if a strong coupling laser or weak probe pulses ( $N_{\text{photons}} \ll N_{\text{atoms}}$ ) are used. Here,  $\delta$  is the probe laser detuning,  $\Omega_c$  the Rabi-frequency of the coupling laser,  $\Gamma$  the spontaneous emission rate between the excited state and the respective ground state,  $\gamma$  the collisional decay rate between the two ground states and  $|\mu|$  the dipole matrix element between the ground and the excited state.

Due to the large Zeeman-shift, the  $\sigma^-$ -polarized beam does not fulfill the Raman-condition and thus its susceptibility can be described by the two-level atom. As can be seen in figure 3, one has to sum over the susceptibilities of all four independent two-level systems, that can interact with the beam. Due to the large detuning from resonance, absorption can be neglected ( $< 0.04\%$  in our system), but the phase shift can become considerable. The susceptibility is then described by [15]

$$\chi^{(-)} = \sum_{j=1}^4 \frac{|\mu_j|^2 \varrho_j}{\hbar \epsilon_0} \frac{\Delta_j + i\frac{\Gamma}{2}}{(\frac{\Gamma}{2})^2 + \Delta_j^2}. \quad (3)$$

Here,  $\varrho_j$  are the populations in the respective ground states,  $\mu_j$  the dipole matrix elements and  $\Delta_j$  the detunings relative to the respective transition, while the decay rate  $\Gamma$  is the same for all of them. The detunings  $\Delta_j$  also depend on the probe detuning  $\delta$ .

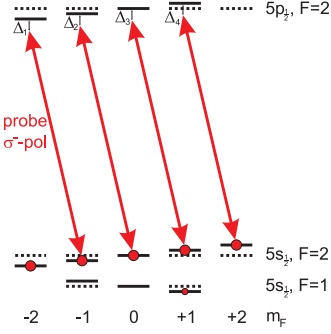


FIG. 3: Level scheme for the  $\sigma^-$ -polarized component of the probe light: the detunings of the respective transitions  $j$  are marked as  $\Delta_j$ .

The electric output field is then given by

$$\begin{aligned}
 |E_{out}|^2 &= |E_{out,\sigma^+} + E_{out,\sigma^-}|^2 \\
 &= \left| \sqrt{1-a^2} E_0 \exp\{i\chi^{(+)} kz/2\} \right. \\
 &\quad \left. + a E_0 \exp\{i\phi\} \exp\{i\chi^{(-)} kz/2\} \right|^2 \\
 &= a^2 \exp\{-\text{Im}\chi^{(-)} kz\} \\
 &\quad + (1-a^2) \exp(-\text{Im}\chi^{(+)} kz) \\
 &\quad + 2a\sqrt{1-a^2} \exp\left\{-(\text{Im}\chi^{(-)} + \text{Im}\chi^{(+)} )kz/2\right\} \\
 &\quad \times \cos\left\{\phi + (\text{Re}\chi^{(-)} - \text{Re}\chi^{(+)} )kz/2\right\}. \quad (4)
 \end{aligned}$$

It can be seen that the first two terms of the equation describe the usual behavior, described the respective susceptibility, while the last term is responsible for the interference and results in the appearance of the dispersive properties of the medium.

Together with equations 1 and 2, this yields the total transmission through the medium via

$$T(\delta) = \frac{|E_{out}|^2}{|E_{in}|^2}. \quad (5)$$

Because we are probing the sample with relatively short pulses, the pulse length limits the minimal EIT bandwidth. The Gaussian pulses are defined as

$$I(t) = I_0 \exp\left\{-\frac{t^2}{\tau^2}\right\}. \quad (6)$$

To include this limitation, one has to evaluate the convolution integral over the Fourier transformed of the Gaussian pulse

$$F(\delta) = \int_{-\infty}^{+\infty} I(t) \exp\{i2\pi\delta t\} dt = \sqrt{\pi}\tau \exp\{-\pi^2\tau^2\delta^2\}, \quad (7)$$

which finally yields the transmission through the cloud:

$$T_P(\delta) = \int_{-\infty}^{+\infty} T(\delta') F(\delta - \delta') d\delta' \quad (8)$$

Unfortunately, there is no analytic solution to this integral.

## EXPERIMENTAL RESULTS

We have measured the EIT-resonance spectrum for three different lengths of the probe pulse:  $\tau = 5\mu\text{s}$ ,  $\tau = 20\mu\text{s}$  and  $\tau = 100\mu\text{s}$ . Figure 4 shows the data of one measurement with a pulse length of  $20\mu\text{s}$  and a coupling laser Rabi-frequency of  $1200\text{ kHz}$ . In this measurement, it can be seen, that the signal contains an absorptive (the peak itself) as well as a dispersive (the asymmetry) part.

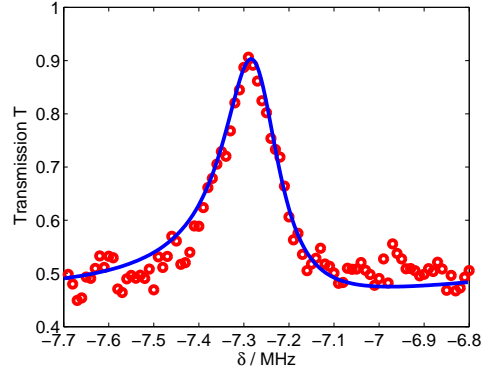


FIG. 4: Transmission spectrum of a  $20\mu\text{s}$  pulse at a coupling laser Rabi-frequency of  $1200\text{ kHz}$ . The absorptive and dispersive parts in the signal can be recognized. The frequency offset of  $\delta_0 = -7.27\text{ MHz}$  corresponds to the differential quadratic Zeeman shift between the two ground state levels. This offset does not depend on the lasers and can thus be used to calibrate the magnetic offset field. For the fit we used equation 5 as an approximation.

The value for the phase  $\phi = 4.95$  was obtained from the fits of all measurements. The curve was fitted with equation 5 and yielded  $\sigma = 100\text{ kHz}$ ,  $\gamma = 8\text{ kHz}$  and  $\delta_0 = 7.27\text{ MHz}$  for the frequency offset due to the quadratic Zeeman shift. The ground state decay rate  $\gamma$  usually corresponds to collisions between the atoms as well as collisions with the background gas. The collision rate rate can usually be neglected, especially in case of large coupling laser Rabi-frequencies. But it can also correspond to a transient effect: for low coupling laser Rabi-frequencies, a steady state in the atomic population cannot be reached within the time of a short probe pulse. This effect shows the same empiric behavior as the collisional loss of polaritons and leads to non-negligible

values of  $\gamma$ .

The data in figures 5 and 6 show the results of the measurements with the  $5\ \mu\text{s}$  and the  $20\ \mu\text{s}$  pulses. For large coupling laser Rabi-frequencies, the coupling laser broadens the line width, while for lower Rabi-frequencies, the pulse length is the limiting factor.

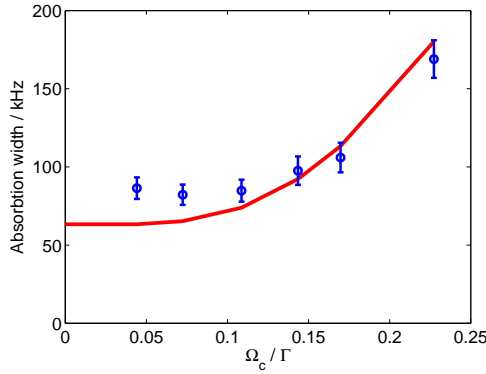


FIG. 5: Theory curve and EIT measurement with  $5\ \mu\text{s}$  pulses. The figure shows the transparency width (Gaussian  $1/e$ -radius) depending on the Rabi-frequency of the coupling laser. The probe pulses contain  $3 \cdot 10^5$  photons within the size of the cloud, which correspond to a maximum Rabi-frequency of  $190\ \text{kHz}$ . The errorbars reflect the uncertainty in the phase  $\phi$ .

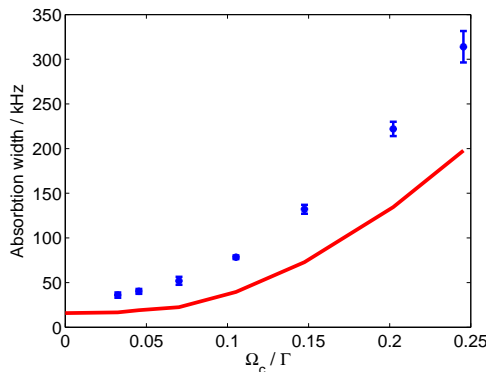


FIG. 6: Theory curve and EIT measurement with  $20\ \mu\text{s}$  pulses. The figure shows the transparency width (Gaussian  $1/e$ -radius) depending on the Rabi-frequency of the coupling laser. The pulses contain  $2 \cdot 10^6$  photons within the size of the cloud, which correspond to a maximum Rabi-frequency of  $220\ \text{kHz}$ . The width is much narrower than the one of the  $5\ \mu\text{s}$  pulses.

The solid curves show the line width that should in theory be obtainable with our setup. For large Rabi-frequencies applied on  $5\ \mu\text{s}$  probe pulses, the measurements are in good accordance with the theory. For all others, the measured line widths are broader than the theory for an

optical density of 0.76 predicts. We attribute these small discrepancies to a decrease in the optical density of the trapped cloud during the experimental measurements. Smaller optical densities can be caused by a reduced number of optically trapped atoms, which is typically observed in the course of the day, and lead to broader theoretically expected line widths. The theory curve is plotted for an optical density of 0.76.

The lack of sufficient coupling light results in an incomplete transparency and limits the relative depth of the EIT dip in the signal. This can be seen in figure 7.

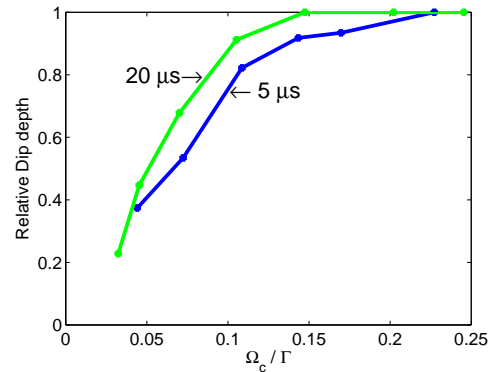


FIG. 7: EIT measurement with  $5\ \mu\text{s}$  and the  $20\ \mu\text{s}$  pulses. The figure shows the relative depth of the EIT dip depending on the Rabi-frequency of the coupling laser. The decrease for small Rabi-frequencies corresponds to the transient effect that a steady state cannot be reached here within the time of a short probe pulse.

To obtain a very narrow line width, a measurement was made with  $100\ \mu\text{s}$  long pulses, containing  $3.9 \cdot 10^6$  photons within the size of the cloud, which corresponds to a maximum Rabi-frequency of  $360\ \text{kHz}$ . Figure 8 shows the result for a coupling laser Rabi-frequency of  $590\ \text{kHz}$ . For lower values, the induced transparency was too low. Due to inefficient EIT, the absorptive part is so low that it is not visible anymore. Instead, due to a large phase shift, the dispersive part of the signal gets enhanced, compared to the measurements shown before.

To enhance the dispersive effect, the  $\sigma^-$ -intensity admixture  $a^2$  was increased to 25 %, which also resulted in a different differential phase shift  $\phi = 4.1$ . With a Gaussian  $1/e$ -half width of  $4\ \text{kHz}$ , this is to our knowledge the narrowest EIT signal measured in ultracold atoms [16, 17]. Narrower signals of  $\sim 30\ \text{Hz}$  have been measured in buffer gas cells, where one is not limited by pulse lengths [18, 19].

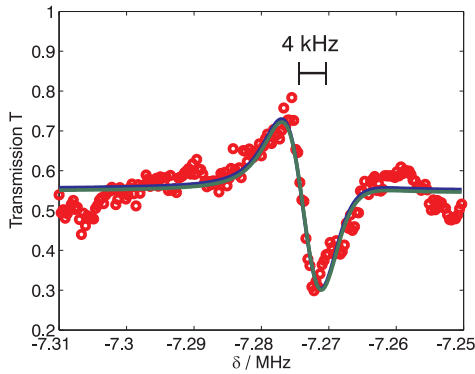


FIG. 8: EIT measurement with a  $100\ \mu\text{s}$  pulse: the line width was reduced to 4 kHz. The transparency is so low that only the dispersive part of the signal can be recognized.

## CONCLUSION AND OUTLOOK

We have shown results on measuring electromagnetically induced transparency (EIT) in pure optically trapped rubidium atoms. The signals yield absorptive and dispersive properties of the atomic medium at the same time. Furthermore, we have measured the narrowest EIT line width in ultracold atoms.

This experiment is an important step towards polarization-dependent long time storage of quantum information in an atomic cloud and the investigation of trapped dark state polaritons.

In our measurements we are still limited by the relatively low optical density of 0.7. The next step will be to optimize the cooling schemes and therefore increase the optical density. This will result in an enhanced atom-light interaction, required for better quantum information processing experiments.

## ACKNOWLEDGEMENTS

We gratefully acknowledge the support of the Alexander von Humboldt foundation and the Landesstiftung

Baden-Württemberg.

---

\* Electronic address: b.kaltenhaeuser@physik.uni-stuttgart.de  
 † URL: <http://www.pi5.uni-stuttgart.de>

- [1] S. E. Harris, J. E. Field, and A. Imamoglu, Phys. Rev. Lett. **64**, 1107 (1990).
- [2] M. Fleischhauer and M. D. Lukin, Phys. Rev. Lett. **84**, 5094 (2000).
- [3] L. Karpa and M. Weitz, Nature Physics **2**, 332 (2006).
- [4] E. Knill, R. Laflamme, and G. J. Milburn, Nature **109**, 46 (2001).
- [5] C. Liu, Z. Dutton, C. H. Behroozi, and L. V. Hau, Nature **409**, 490 (2001).
- [6] D. F. Phillips, A. Fleischhauer, A. Mair, R. L. Walsworth, and M. D. Lukin, Phys. Rev. Lett. **86**, 783 (2001).
- [7] M. S. Bigelow, N. N. Lepeshkin, and R. W. Boyd, Science **301**, 200 (2003).
- [8] L.-M. Duan, M. D. Lukin, J. I. Cirac, and P. Zoller, Nature **414**, 413 (2001).
- [9] A. Kuzmich, L. Mandel, and N. P. Bigelow, Phys. Rev. Lett. **85**, 1594 (2000).
- [10] J. M. Geremia, J. K. Stockton, and H. Mabuchi, Science **304**, 270 (2004).
- [11] J. Hald, J. L. Sørensen, C. Schori, and E. S. Polzik, Phys. Rev. Lett. **83**, 1319 (1999).
- [12] S. R. de Echaniz, M. W. Mitchell, M. Kubasik, M. Koschorreck, H. Crepaz, J. Eschner, and E. S. Polzik, J. Opt. B **7**, S548 (2005).
- [13] G. T. Purves, C. S. Adams, and I. G. Hughes, Physical Review A **74**, 023805 (pages 4) (2006).
- [14] M. Fleischhauer, A. Imamoglu, and J. P. Marangos, Rev. Mod. Phys. **77**, 633 (2005).
- [15] D. Suter, *The Physics of Laser-Atom Interactions* (Cambridge University Press, 1997).
- [16] L. V. Hau, S. E. Harris, Z. Dutton, and C. H. Behroozi, Nature **397**, 594 (1999).
- [17] D. A. Braje, V. Balic, S. Goda, G. Y. Yin, and S. E. Harris, Physical Review Letters **93**, 183601 (pages 4) (2004).
- [18] S. Brandt, A. Nagel, R. Wynands, and D. Meschede, Phys. Rev. A **56**, R1063 (1997).
- [19] M. Erhard, S. Nußmann, and H. Helm, Phys. Rev. A **62**, 061802(R) (2000).